International Journal of Heat and Mass Transfer 52 (2009) 3654–3664

Contents lists available at ScienceDirect

International Journal of Heat and Mass Transfer

journal homepage: www.elsevier.com/locate/ijhmt

Film cooling at hypersonic Mach numbers using forward facing array of micro-jets

R. Sriram, G. Jagadeesh *

Department of Aerospace Engineering, Indian Institute of Science, Bangalore, Karnataka 560012, India

ARTICLE INFO

Article history:
Received 25 June 2008
Received in revised form 22 January 2009
Accepted 6 February 2009
Available online 11 April 2009

Keywords:
Hypersonic flow
Film cooling
Forward facing jet/micro jets

ABSTRACT

Experimental investigations are carried out in the IISc hypersonic shock tunnel on film cooling effectiveness of a single jet (diameter 2 mm and 0.9 mm), and an array forward facing of micro-jets (diameter 300 μm each) of same effective area (corresponding to the respective single jet). The single jet and the corresponding micro-jets are injected from the stagnation zone of a blunt cone model (58° apex angle and nose radius of 35 mm). Nitrogen and Helium are injected as coolant gases. Experiments are performed at freestream Mach number 5.9, at 0° angle of attack, with a stagnation enthalpy of 1.84 MJ/kg, with and without injections. The ratios of the jet stagnation pressure to the freestream pitot pressure used in the present study are 1.2 and 1.45. Up to 50% reduction in surface heat transfer rate was observed with the array of micro-jets, compared to that of the respective single jet with nitrogen as the coolant, while the corresponding reduction was up to 37% for helium injection, with the schlieren flow visualizations showing no major change in the shock standoff distance, and thus no major changes in other aerodynamic aspects such as drag.

1. Introduction

Large angle blunt cones are extensively used in hypersonic missions so as to bring down the high aerodynamic heating, with the cost being paid on increased drag [1]. Even with the use blunt cones the heat transfer in the nose region, where the flow almost stagnates, is high enough that conventional materials cannot withstand the associated high temperatures. The safety of the hypersonic vehicles is thus ensured by providing appropriate thermal protection system (TPS). Injection of a mass of cold fluid into the boundary layer through the surface is a potential cooling technique, which includes "transpiration cooling" (injection through porous media) and "film cooling" (injection through slots as jets) [6].

A number of investigations on hypersonic drag reduction using high momentum jets from stagnation point of a blunt body (that can push the bow shock away from the body) have been reported in open literature [2–4] where the heat transfer rates are reduced over most parts of the surface except in the region around the jet reattachment where the reattachment shock invariably increases local heat flux. Thus lower momentum fluxes of the coolant are preferred for film cooling [5,6]. Thus it is known from literature that the film cooling gets better with mass flow rate of the jet, but the higher momentum flux can lead to a stronger jet reattachment on the surface thus locally increasing the heat transfer rates. If we are able to reduce the jet momentum flux for the same mass flow rate, the gas coming out of the jet can easily spread over the boundary layer and it is possible to achieve better film cooling. It is in this background that the current investigation has been done, where the reduction in momentum of the coolant jet is achieved by injecting the coolant mass through an array of closely spaced small orifices rather than through a single orifice of the same area as that of the array of orifices. In the previous works from our lab [3,6], the injection was through a single orifice, and the stagnation pressure of the jet was not measured. The reported total pressure characterizing injection was the pressure in the gas cylinder from which the injected mass is admitted. With the changes in the valves and pipes used for injection it is not possible to take those results for the comparison with the current set of experiments as the pressure losses are different. Hence experiments are also done with a single jet so that comparison with the corresponding array can be made for same total pressure of injection. In the current work the total pressure of the injected mass is measured using a PCB pressure sensor located in stagnation chamber inside the blunt cone model just before the injection orifice.

2. Physical picture of the flow field and dimensional analysis

When the mass of cold fluid is injected with low momentum flux it cannot carry forward for a long distance and affect the structure of the outer flow field, but fills the boundary layer. Fig. 1 shows the typical flow topology with low momentum injection with a single jet and with an array of micro-jets.

The injected mass carries forward till distance from the orifice and then is deflected back and reattaches on the surface of the body leaving a region of dead air as in Fig. 1. With low momentum

* Corresponding author. Tel.: +91 80 22933030; fax: +91 80 23606250.
E-mail address: jaggie@aero.iisc.ernet.in (G. Jagadeesh).

0017-9310/$ - see front matter © 2009 Elsevier Ltd. All rights reserved.
doi:10.1016/j.ijheatmasstransfer.2009.02.035

Nomenclature

c_p	specific heat at constant pressure (J kg^{-1} K^{-1})
D	binary diffusion coefficient (cm^2 s^{-1})
d_j	orifice exit diameter of the jet/micro jets (mm)
d_l	distance between individual micro jets (neighboring) in the array (mm)
K	ratio of reduction in heat transfer rate to heat transfer rate without injection
L	shock standoff distance (mm)
M	Mach number
P	pressure ratio = P_{oj}/P_{of} (also called stagnation pressure ratio)
P_{of}	pitot pressure of freestream (Pa)
P_{oj}	total pressure of the jet/array of micro jets (Pa)
Pr	Prandtl number
q_t	surface heat transfer rate (W cm^{-2} or W m^{-2})
R	Reynolds number
Rn	nose radius of the blunt cone (mm)
S	distance along the model surface from stagnation point (mm)
Sc	Schmidt number
St	Stanton number
St_{rp}	percentage reduction in Stanton number
T	stagnation temperature ratio = T_{oj}/T_{of}
T_o	stagnation temperature of freestream (K)
T_{oj}	stagnation temperature of the jet/array of micro jets (K)
T_w	wall temperature (K)
U	jet exit velocity (m s^{-1})
u_∞	freestream velocity (m s^{-1})

Greek symbols

α	thermal diffusivity
γ	ratio of specific heats at constant pressure and constant volume
μ	coefficient of viscosity (N s m^{-2})
ρ	density (kg m^{-3})

Subscripts

j	jet exit condition
o	stagnation condition
∞	freestream condition

the injected mass is confined within the bow shock. With a single jet the point of reattachment is far away from the injection point compared to the corresponding array of closely spaced micro-jets with same injection pressure. Also the reattachment with the single jet is characterized by higher velocities owing to its higher momentum. But with the array of micro-jets the reduction in momentum flux due to the interaction between individual jets and also due to the lower orifice diameters, makes the coolant mass almost spread over the surface as soon as it is injected. If the jets are closer the dead air region is smaller and the reattachment is weaker, with other conditions being the same.

For given freestream conditions the reduction in surface heat transfer rate at any location on the surface due to the mass injection as a jet or array of jets is dependent on mass flow rate of the coolant, momentum flux of the coolant at orifice exit, temperature of the coolant, ratio of specific heats γ of the coolant, the ability of the coolant to diffuse into the boundary layer, interaction between the jets (for array of micro-jets).

The mass and momentum flow rates are specified with the exit area, average velocity U and density ρ of the jet(s) at the exit. The ability of the coolant to diffuse into the boundary layer is given by the binary mass diffusion coefficient D, which is dependent on the molecular masses of the freestream gas and of the coolant. The interaction between the jets is specified by the distance between the orifices d_l and the viscosity. T_j is the jet exit temperature. If K is taken as the ratio of reduction in heat transfer rate with mass injection to the heat transfer rate without injection, then from dimensional analysis (assuming the coolant and freestream gases are perfect gases)

$$K = f(R_j, R_1, M_j, Sc, Pr, \gamma) \tag{1}$$

where $R_j = \rho U d_j/\mu$ is Reynolds number based on jet exit diameter, $R_1 = \rho U d_l/\mu$ is Reynolds number based on distance between the orifices, M_j is the jet exit Mach number, $Sc = \mu/\rho D$ is the Schmidt number, $Pr = \mu/\rho\alpha$ is the Prandtl number where α is the thermal diffusivity.

Since it is difficult to measure the jet properties at the exit during the run time, an alternate way of specifying the factors influencing the reduction in heat transfer is being looked at. The reduction in heat transfer rate can be related to the controlling parameters that dictate the jet exit conditions for given freestream conditions. The mass flow rate of the coolant is dependent on the pressure difference that drives it, the net area A_{tj} of the orifice(s) from which the jet issues and on the viscosity μ of the coolant. The momentum flow rate is also dependent on viscosity and on the pressure difference, but for each of the jet it is dependent on the diameter of the orifice d_j. For the entire array, the momentum flux is also dictated by the viscous interaction between the jets, specified by d_l. The jet exit temperature is dependent on the jet stagnation temperature T_{oj}. P_{oj} is the coolant stagnation pressure and P_{of} is the pitot pressure of freestream.

It is also expected that keeping the effective area of injection the same, splitting a single jet injection area into a number of smaller areas of injection does not alter the mass flow rate, for other conditions being the same, although it may alter the momentum flow rate to some extent. With an orifice having small thickness, the flow will not be fully developed. The average velocity at any section of the orifice is a little lesser than the core velocity due to the thin (compressible) boundary layer flow. By decreasing the orifice diameter for the same thickness, the viscous effects increase, and the core flow diameter reduces. But still for the orifice thickness of 2 mm and diameter of 0.3 mm the boundary layer is thin, and so does not alter the average velocity much. As mass flow rate u, momentum flow rate u^2, where u is some characteristic velocity, it is a fair expectation that the by splitting a single jet into a number of smaller jets, issuing out from the same effective area, with other conditions being the same, difference in mass flow rate is negligible. But the difference in the momentum flow rate can be considerable. Thus for a given mass flow rate, for a given coolant fluid, the momentum flow rate at orifice exit is specified by diameter of orifice d_j. The mass flow rate is specified by the stagnation pressure P_{oj} of the jet for given freestream conditions and for given effective area of injection. Normalizing pressure using freestream pitot pressure P_{of}, temperature using freestream stagnation temperature T_o, and the length scales using the nose radius of the model Rn, the percentage reduction St_{rp} in Stanton number (heat transfer rate normalized with freestream conditions) can be written as,

$$St_{rp} = F(P, T, d_j/Rn, dl/Rn, Sc, Pr, \gamma) \tag{2}$$

where $St_{rp} = \{[(St)_{\text{with injection}} - (St)_{\text{without injection}}]/(St)_{\text{without injection}}\} * 100\%$, $P = P_{oj}/P_{of}$ is the jet stagnation pressure ratio, or simply the pressure ratio, $T = T_{oj}/T_o$ is the jet stagnation temperature ratio.

In the current investigation, the effect of P, d_j/Rn, d_l/Rn and Sc on heat transfer reduction is studied by keeping the freestream conditions the same. Though surface roughness is one other parameter that can affect the phenomenon (when the flow field can become turbulent), it is not within the scope of the current investigation. However in the present study the hypersonic flow over the blunt cone is laminar.

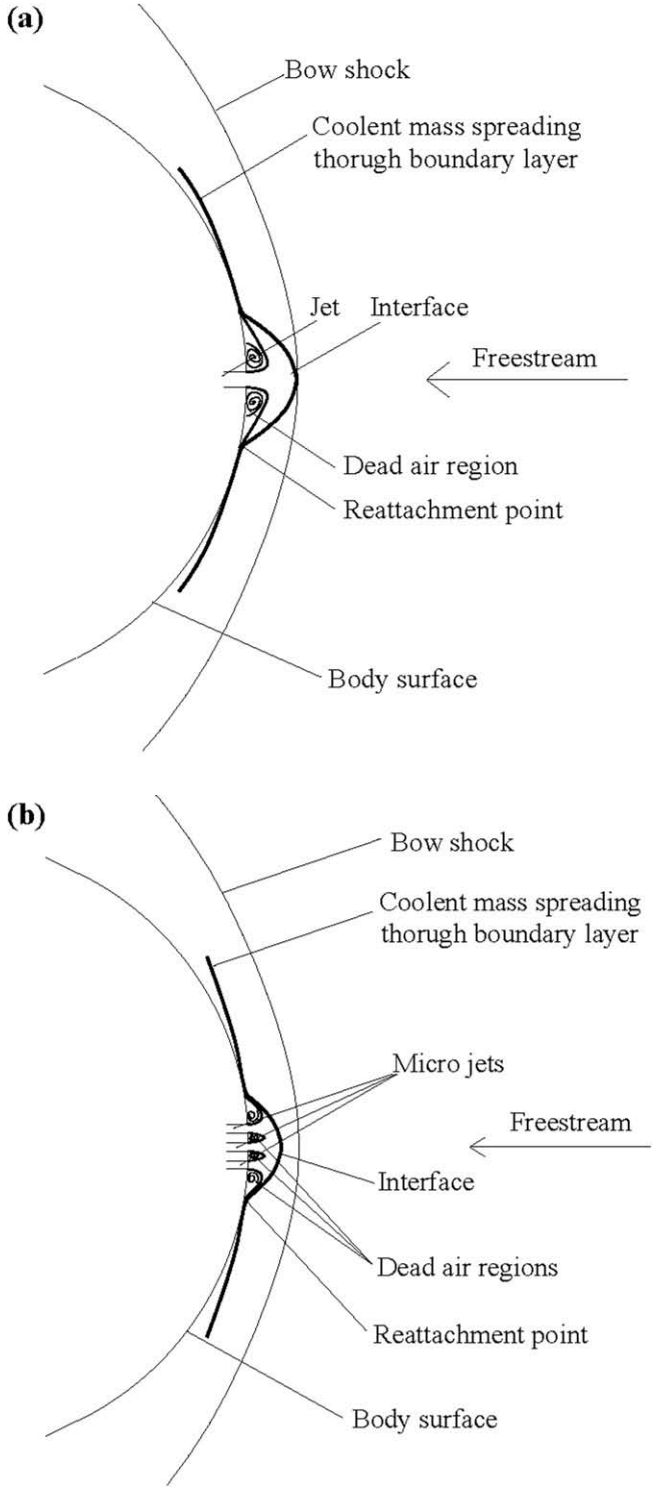

Fig. 1. Schematic diagram showing the flow topology over the blunt cone with low momentum counter flow injection: (a) with a single jet, (b) with array of micro jets.

3. Experimental facility and test model

All experiments in the present study are carried out in IISc hypersonic shock tunnel HST2 [6]. This tunnel can be operated in straight through mode or reflected mode with a Mach number range of 5.75–12 and simulate flow enthalpy up to 5.0 MJ/kg. It consists of a conical nozzle of 300 mm exit diameter. The hypersonic flow from this nozzle goes through a rectangular test section of 300 mm × 300 mm cross section and 450 mm length to a dump tank having a volume of 1 m^3. The driver and driven sections of the shock tube are separated by a metallic diaphragm of appropriate thickness and the shock tube and the nozzle are separated by a thin paper diaphragm. The flow Mach number in the test section is varied by changing the throat portion of the nozzle.

The test model is a 58° apex angle blunt cone of nose radius 35 mm with base diameter 80 mm. The nose of the cone has a square slot of 13 × 13 mm^2 area and thickness 2 mm where the plate containing orifice(s) is placed. For single jet injection plates with single orifice of 2 mm and 0.9 mm diameter are used. For the array of micro jets corresponding to 2 mm diameter jet, plate with 46 orifices (arranged more or less square), each of 300 μm, confined within 5 × 5 mm^2 is used. Corresponding to 0.9 mm jet, plates with 9 orifices of 300 μm, with one in which the orifices are confined within 5 × 5 mm^2 and the other within 3 × 3 mm^2 are used. The array of orifices has more or less the same effective area as that of the corresponding single jet orifice (area of 45 orifices of 300 μm almost equals the area of 2 mm orifice and of 9 orifices of 300 μm equal area of 0.9 mm orifice). The coolant gas settles in a stagnation chamber inside the model from where it is injected through the orifice. The jet stagnation pressure is measured in the stagnation chamber. The coolant gas is admitted from the gas cylinders through a solenoid valve during the run time [3]. For experiments without injection, the orifice plate is replaced with a plate without any orifice to avoid any cavity effect. Fig. 2 shows the photograph of the model.

4. Shock tunnel experiments

The tunnel is operated in straight through mode. A pitot probe is placed to measure the freestream stagnation pressure behind the normal shock. The diaphragm rupture pressure and the nozzle chamber pressure in the shock tube are noted during each run. The coolant is injected during the run time with the help of a solenoid valve. The stagnation pressure of the coolant is measured by means of a PCB pressure transducer at the stagnation chamber in the model. Two to three experiments are done for each condition to check the repeatability of the signals. The repeatability of the experiments is critically determined by the consistency in the rupture pressure of the diaphragms and hence is monitored with care. The repeatability of the freestream conditions can be established by comparing the pitot signals of all the experiments. Fig. 3 shows the repeatability in pitot signals for four runs of the tunnel. The freestream conditions are estimated from the average value of the signals (pitot and other measured shock tube condition) during the test time. The average of the estimated freestream conditions (of all runs) is shown in Table 1. The uncertainties in measurements are obtained from the standard deviation in the measured value during test time. The other freestream uncertainties are then obtained from the measured uncertainty values [11]. Test time is estimated from the pitot signal as shown in Fig. 3. The IISc hypersonic shock tunnel HST2 being impulse facility has test time of ~500 μs. Although the pitot signal is steady for a longer time (around 500 μs), with jet injection a conservative estimate of the test time (around 300 μs) is considered in the present study to take into account the establishment of the flow of the injected gas over

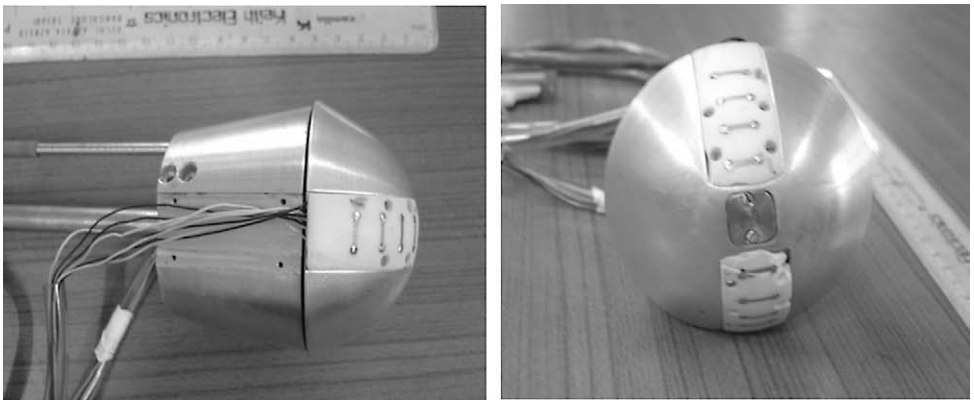

Fig. 2. Photograph of the model with platinum thin film sensors and orifice plate of 46 orifices of 300 μm.

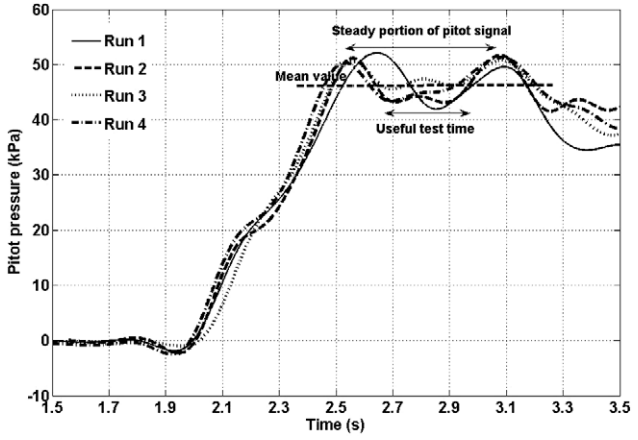

Fig. 3. Repeatability of pitot signals – typical pitot signals for four runs with the indication of useful test time.

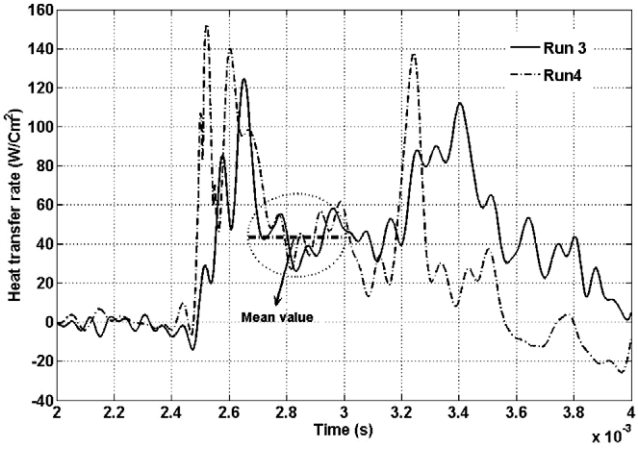

Fig. 4. Repeatability of the heat transfer signals – typical heat transfer rate signals for two runs at $S/Rn = 0.46$, with injection of nitrogen as array of 46 micro jets with $P = 1.2$.

Table 1
Freestream conditions.

Freestream condition	Value
Freestream Mach number M_∞ (±0.4%)	5.9
Stagnation enthalpy H_o (MJ/kg) (±1%)	1.84
Stagnation pressure P_o (KPa) (±2%)	1443
Freestream static pressure P_∞ (KPa) (±3.4%)	1.013
Freestream static temperature T_∞ (K) (±1.3%)	230
Freestream unit Reynolds number Re_∞ (/m) (±3.7%)	1.023×10^6

the surface (this could be seen in the first 200 μs after the rising of heat transfer signal in Fig. 4). Thus for heat transfer signal too the corresponding time is taken for obtaining the mean heat transfer rate value as discussed in subsequent section.

4.1. Heat transfer measurements

The convective heat transfer rates over the test model are measured by platinum thin film gauges. These thin film sensors are sputtered on Macor strips placed symmetrically on the model in the slots cut on either side of the injection zone. Provision is made through the slots to take the electrical leads. The sensors are powered with constant current sources and connected to PC-based data-acquisition system. The change in voltage across the gauge with respect to time gives the temperature–time history at the gauge location on the model surface. These temperature signals are then numerically integrated in order to get the convective surface heat transfer rate [9,10]. Fig. 4 shows the typical heat transfer signals for 2 experiments with array of 46 micro jets with same injection pressure ($P = 1.2$) at the sensor located closest to the stagnation point ($S/Rn = 0.46$). The average value during the test time is taken as representative heat transfer value (whether the signal is steady or unsteady during test time). The average value of heat transfer rate during the test time for the representative signals is also shown in Fig. 4 with a broken line. The surface heat transfer rates are measured with and without injection of the coolant gas. Generally the heat transfer rates show unsteadiness with gas injection for the sensors located near the stagnation point, but become steady far away. Without injection the heat transfer rates are fairly steady for all sensors. A comparison between the heat transfer rate signals for cases without injection, with single jet from 2 mm orifice and with corresponding array of 46 micro jets ($P = 1.2$ for both injections) is shown in Fig. 5. The test time during which the heat transfer rate values are noted is highlighted. The highlighted portion is magnified in Fig. 5(b). It can be seen that heat transfer rate is not just statistically lesser for the case of array of micro jets as compared to the other cases, but also is lesser throughout the test window. The variation of the heat transfer rates along the surface of the blunt cone model for the above cases is shown in Fig. 6.

4.2. Schlieren visualization

Time resolved schlieren flow visualization of the blunt body hypersonic flow field is carried out using high speed camera. The

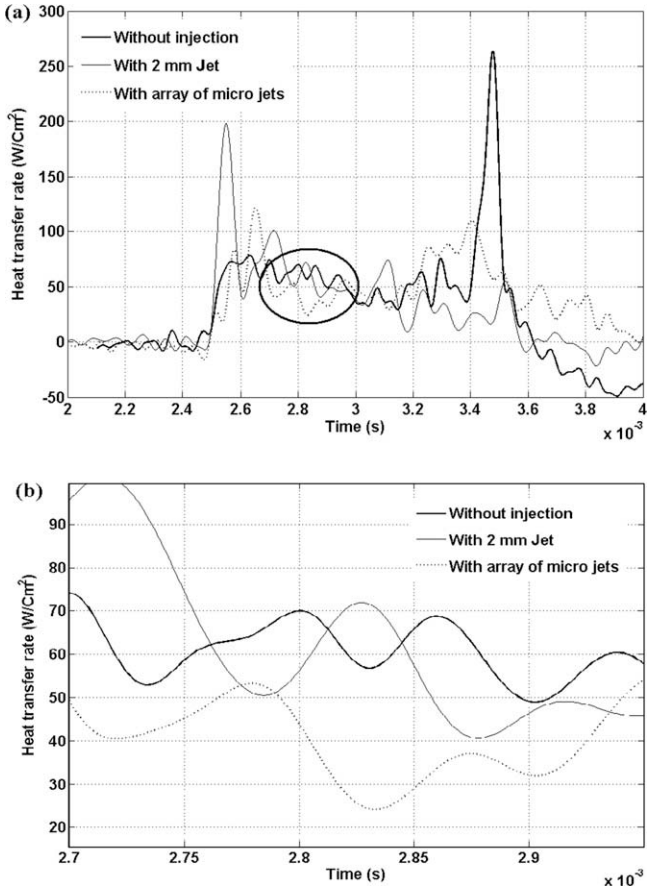

Fig. 5. Comparison of heat transfer rate signals at $S/Rn = 0.46$ with and without injection of nitrogen with $P = 1.2$: (a) with the test time highlighted, (b) with the portion of the signal during the steady time magnified.

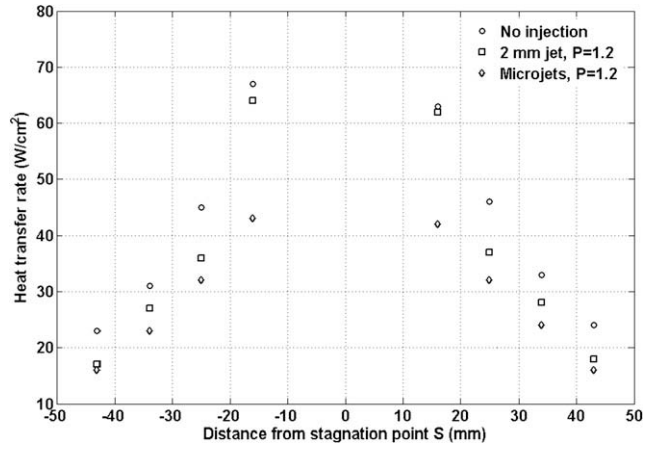

Fig. 6. Variation of heat transfer rate over the 58° apex angle blunt cone surface along the distance measured from the stagnation point with and without injection ($P = 1.2$ and injection through 2 mm orifice and corresponding micro orifices).

shock standoff distance is an indicator of the qualitative changes in the aerodynamic characteristics (like drag) due to mass injection. For visualizing the flow field pattern schlieren imaging technique is used in a 'z-type' set-up. For the present set of experiments the camera (Phantom 7.2 high speed camera, Ms. Vision Research, USA) is operated at 10,000 frames per second with a resolution of 450 × 450 pixels. A standard 300 W North star lamp with C-clamp base is used as a continuous light source. Operation of the camera is synchronized with the shock tunnel flow using a trigger pulse generated by the pressure sensor located at the end of the tube. The light is switched on just before the experiment and the camera is triggered to synchronize with the shock tunnel flow. The camera is focused on the region of interest. For details on the operational procedures of the camera see [12]. The shock stand of distance is measured from the visualizations for all experiments for all frames during the steady time, at the stagnation point and at the locations of the heat transfer sensors.

4.3. Measurement uncertainties

The uncertainties in the freestream conditions are given in Table 1. The uncertainties in the measured heat transfer rates are dependent on error in the output of the data-acquisition system (±1.99%), error in the thin film gauge backing material (Macor) property β (±2.5%), error in temperature coefficient of resistance α (±1.5%), error in initial voltage from the power supply of gauges (±0.5%), error in voltage gain (±0.4%).

Thus the error in the measured heat transfer rate is estimated to be ±3.59%. From the freestream conditions the Stanton number is estimated to be ±5.3% accurate. The calculations in uncertainties are done based on the method described by Moffat [11].

5. Results and discussions

5.1. Convective surface heating rates

Convective surface heat transfer rates q_t measured at different locations on the blunt cone model are expressed in terms of the ratio of arc length s on the cone surface measured from the geometric stagnation point and nose radius Rn. These convective surface heating rates at all gauge locations are normalized with freestream conditions and are expressed in terms of Stanton number. The Stanton number is expressed as

$$St = \frac{q_t}{\{\rho_\infty u_\infty [c_p(T_o - T_w)]\}} \tag{3}$$

where ρ_∞ and u_∞ are the freestream density and velocity, c_p is the specific heat of air at constant pressure, and T_w is the wall temperature. The variation of convective heat transfer rates expressed in terms Stanton number along the surface of the model with and without coolant gas injection from area corresponding to 2 mm orifice (including single jet and array of micro-jets) at two different stagnation pressure ratios $P = 1.2$ and $P = 1.45$ are shown in Fig. 7(a) and (b). Fig. 7(a) shows the variation of Stanton number along the surface of the test model with nitrogen as coolant gas, and Fig. 7(b) shows for helium as coolant. Shown in these figures are also the Fay and Riddell's stagnation point Stanton number value [7], and the Lee's theoretical Stanton number values [8] for the blunt cone model along the surface. The Fay and Riddell's stagnation point heat transfer value for the model, for the given freestream conditions is 79 W/cm^2. In general, for blunt cone model without any injection, the maximum heating occurs at the stagnation point and decreases gradually along the conical portion of the model. The theoretical value without injection is indicated in the figures by a solid line. In the present model it is not possible to have heat transfer gauge at the stagnation point as the orifice plate is to be mounted. The sensors are placed from the nearest possible location from the stagnation point (from $S/Rn = 0.46$).

Essentially when the coolant gas is admitted from the nose it turns back and flows over the surface. It flows through the boundary layer and reduces the driving temperature difference thereby reducing the heat transfer rates. The percentage reduction in heat transfer rates St_{rp} (in terms of Stanton number) along the model

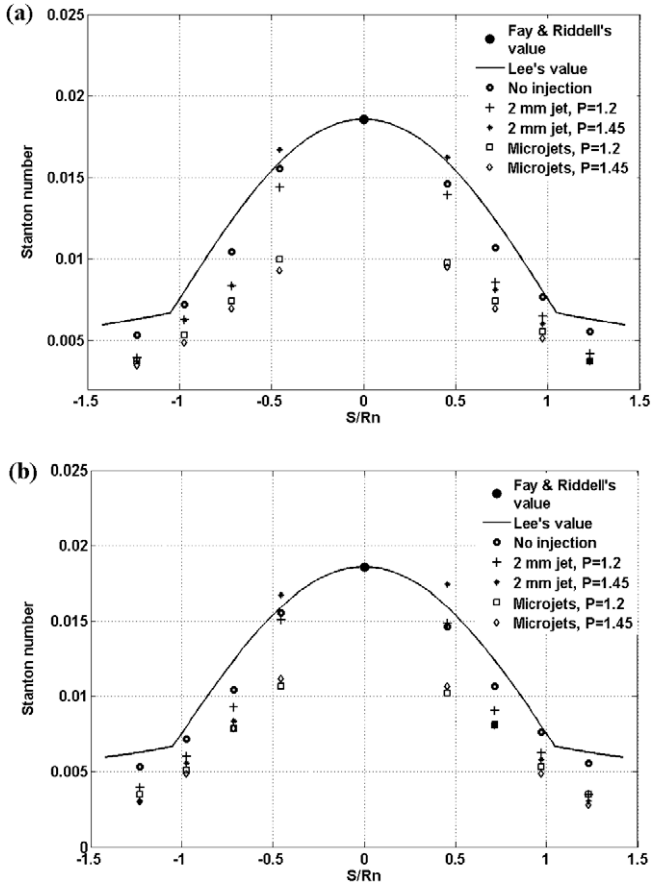

Fig. 7. Variation of Stanton number over the 58° apex angle blunt cone surface at two different pressure ratios: (a) with and without nitrogen injection, (b) with and without helium injection.

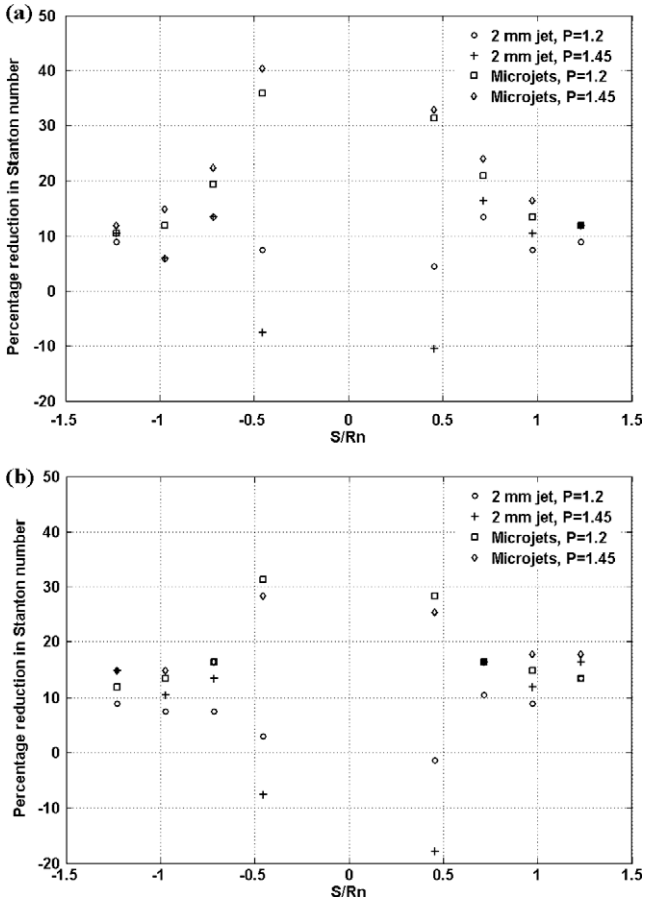

Fig. 8. Percentage reduction in Stanton number over the surface of the 58° apex angle blunt cone model at two different pressure ratios: (a) with nitrogen injection, (b) with helium injection.

surface due to the injection of a single jet (2 mm) and due to the injection of corresponding array of micro-jets at two different pressure ratios are compared in Fig. 8(a) for nitrogen as coolant and in Fig. 8(b) for helium as coolant. More the mass of the admitted coolant, more will be the mass of coolant that flows through the boundary layer, and thus more will be the tendency of heat transfer rates to reduce. But higher momentum flux tends to reduce the effectiveness of film cooling as the laminar convective heat transfer rates increase with increase in momentum. If the mass is injected as a single jet, it will have higher momentum than when it is injected as array of micro-jets with same pressure ratio. The momentum reduction with the array of micro-jets has a major contribution from the viscous interaction between individual jets of the array, and could have a reasonable contribution from the increased viscous effects from the boundary layer on the orifice walls by decreasing the (individual) jet diameter. This jet interaction phenomenon has been explained in subsequent paragraphs with some more experimental results. The single jet having higher injection momentum flux can carry forward as a jet for a longer distance than the corresponding array of micro-jets which almost seem to spread over the surface of the model as soon as it comes out of the orifice (will be discussed in detail showing the visualizations). The mass of the single jet deflected back by the freestream flow reattaches on the model surface leaving a region of dead air from the point of injection to the point of reattachment. In the dead air region considerable reduction in the heat transfer rate is observed. Even though the jet does not push the shock forward it can have a 'strong' reattachment where the jet mass experiences compression. Due to compression the temperature of the jet mass is increased at the point of reattachment. This increases the local heat transfer values. This can be seen in Fig. 9 where the local heat transfer rates at $S/Rn = 0.46$ either have no substantial reduction or have increased when compared to that of without any injection. The heat transfer rates in this location with a single jet are almost close to the heat transfer rates without any jet for $P = 1.2$, but increases by 10% for $P = 1.45$ (almost the same trend for both helium and nitrogen injection). This may be because for the higher pressure ratio the point of reattachment is closer to the sensor (reattachment point is farther from point of injection for higher pressure ratio) than for lower pressure ratio. Also the reattachment is relatively weaker for lower pressure ratio. At the same location for the case of injection of array of micro-jets a reduction in Stanton number of up to 40% is observed with nitrogen as coolant, and up to 30% with helium as coolant.

From the point of reattachment the jet fluid mass starts accelerating over the surface and spreads over the boundary layer. Near the reattachment zone the thickness of the boundary layer is less and the coolant mass accelerates fast, thus has higher momentum. The heat transfer reduction on the surface for a substantial distance from reattachment zone is thus lesser with a single jet, than corresponding array of micro-jets, owing to the higher momentum of the coolant over the surface after reattachment. But as the distance from the reattachment zone increases both single jet and array of micro-jets (for same P) leads to more or less the same reduction, as they have more or less the same temperature, boundary layer thickness and momentum far away from the reattachment zone (of the single jet). This can be seen in Fig. 9 where for $S/Rn = 0.97$ the difference in percentage reduction in Stanton number between

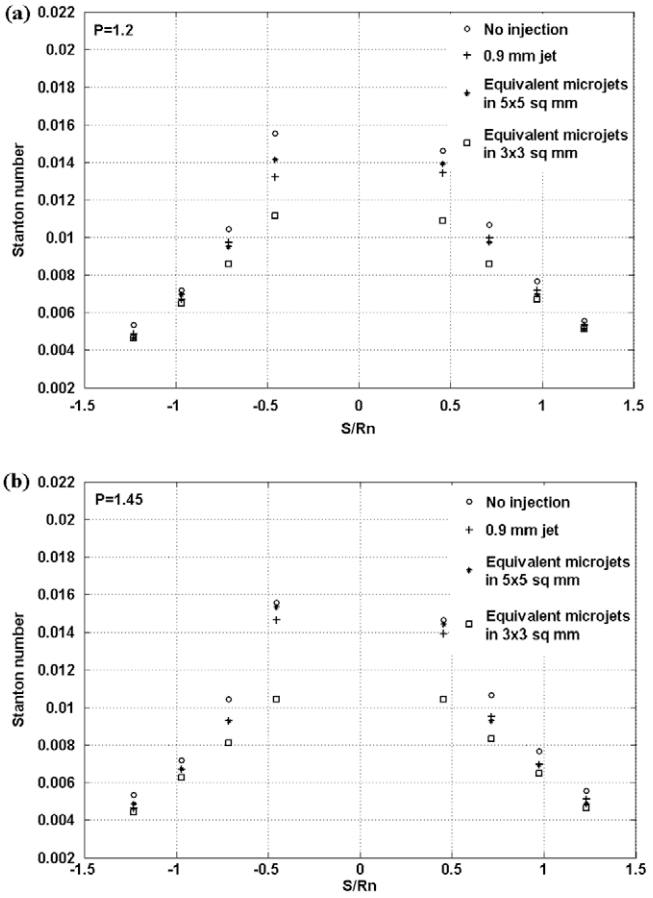

Fig. 9. Variation of the Stanton number over the 58° apex angle blunt cone surface, with and without nitrogen injection, as a single jet (0.9 mm) and as corresponding arrays, with (a) $P = 1.2$, (b) $P = 1.45$.

them is just around 5, and for $S/Rn = 1.23$ it is even (lesser less than 3), although the general trend is increased reduction with array of micro jets, compared to single jet.

5.2. Effect of pressure ratio

The increase in pressure ratio generally increases the percentage reduction in Stanton number, the exception being when $S/Rn = 0.46$. With a single jet this is the reattachment zone. With array of helium micro-jets also the trend is the decrease in heat transfer reduction with increase in P for $S/Rn = 0.46$. Increase in pressure ratio leads to increase in both mass and momentum flow rate of the coolant at the orifice exit. Near the injection zone the momentum of the coolant, spread over the boundary layer can be more for higher pressure ratios. But as the distance from the stagnation point (or reattachment zone in the case of single jet) increases, there is no big difference in momentum of the coolant for different values of P. Thus for higher pressure ratios, away from the stagnation/reattachment zone, because of the effect of higher mass flow rate of the coolant considerable reduction in heat transfer rate is observed.

5.3. Effect of the coolant gas

By changing the injection gas, we essentially change the mass and momentum flow rate and also the diffusion abilities of the coolant. For the same injection pressure and pitot pressure (same P), helium being a lighter gas has lesser mass and momentum flow rate, but has better mass diffusion ability than nitrogen. For a temperature of 250 K the binary mass diffusion coefficient of helium with air is 1.22 cm^2/s, while for nitrogen it is 0.283 cm^2/s, obtained from their molecular weights from Fick's law. Generally when a lighter gas is injected it comes out of the exit plane it diffuses faster along the surface of the body. Thus we have higher reduction in heat transfer rates with nitrogen than for helium for the sensors near the stagnation point (owing to mass flow rate as well). The cooling performance of nitrogen is better in the vicinity of the stagnation point compared with helium. Far away from stagnation point the heat transfer reduction with helium is more than that with nitrogen, but appreciable differences are not observed. Although γ is different for the two gases the difference is not by an order as with the mass diffusion or molecular mass, and thus is not attributed to the differences in film cooling performances here.

5.4. Effect of distance between the jets

Few more experiments have been conducted to confirm the effect of interaction between the jets in the array on the reduction in momentum and hence on the heat transfer reduction. It is not possible to vary the characteristic distance between the jets in the array of 46 micro jets, as increasing the distance could make the array occupy a substantial portion on the model surface and hence making it difficult to measure heat transfer rate close to stagnation region. Also it is not possible to have the jets further closer due to difficulties in fabrication. Hence a 0.9 mm orifice and its equivalent of nine micro jets of 300 μm are chosen. The nine orifices are placed farther in a square of $5 \times 5\ mm^2$ area, and closer in a square of $3 \times 3\ mm^2$ area. The choice of this set also leads to lower mass flow rate, for the same pressure ratio, when compared with that of 2 mm jet and corresponding array, due to lower injection area. Fig. 9 shows the Stanton number as a function of S/Rn for the three cases, one for a single jet injection, one for the injection of the array of closely spaced micro jets (in $3 \times 3\ mm^2$), and the other for the injection of the array of micro jets spread far apart (in $5 \times 5\ mm^2$), for different pressure ratios, with nitrogen as the coolant gas. From the figure it can be seen that with the single jet and with the corresponding array of micro jets from $5 \times 5\ mm^2$ area, the heat transfer values almost remain the same, but with the array from $3 \times 3\ mm^2$ area the values are substantially lower near the stagnation zone, very much like what was observed with the set corresponding to 2 mm jet. But in general, for all cases with the current set of experiments it can be seen that the reduction in Stanton number is not as much as the reduction with the results corresponding to 2 mm jet. This is because of the lower mass flow rate of the coolant for the current set, when compared with the set corresponding to 2 mm jet, with same pressure ratio. Fig. 10 shows the percentage reduction in Stanton number along the surface of the model with nitrogen injection through the current set of jet orifices, for different pressure ratios.

The trend of the reduction with closely spaced jet array almost resembles the 46 micro jets array, but with a lower reduction percentage. The reduction is higher near the stagnation zone and subsequently reduces as we move away from the stagnation zone. With the other cases, the reduction is very low near the stagnation zone, probably due to the sensor being in the vicinity of the reattachment zone. Away from the stagnation zone, due to lower mass flow rates substantial difference in reduction between the three cases cannot be noticed. But what can be confirmed out of this set of experiments is that it is the viscous interaction between the jets in the array, which primarily leads to the reduction in momentum and hence in heat transfer near stagnation zone. Hence the closely spaced jet array has better cooling performance than

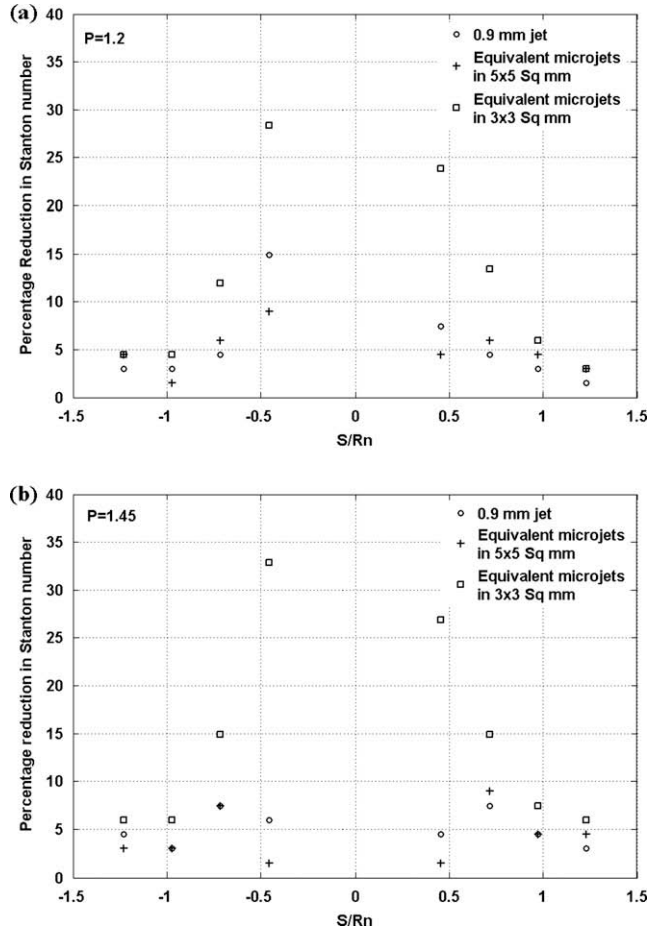

Fig. 10. Percentage reduction in Stanton number over the surface of the 58° apex angle blunt cone model with nitrogen injection, as a single jet (0.9 mm) and as corresponding arrays, with (a) $P = 1.2$, (b) $P = 1.45$.

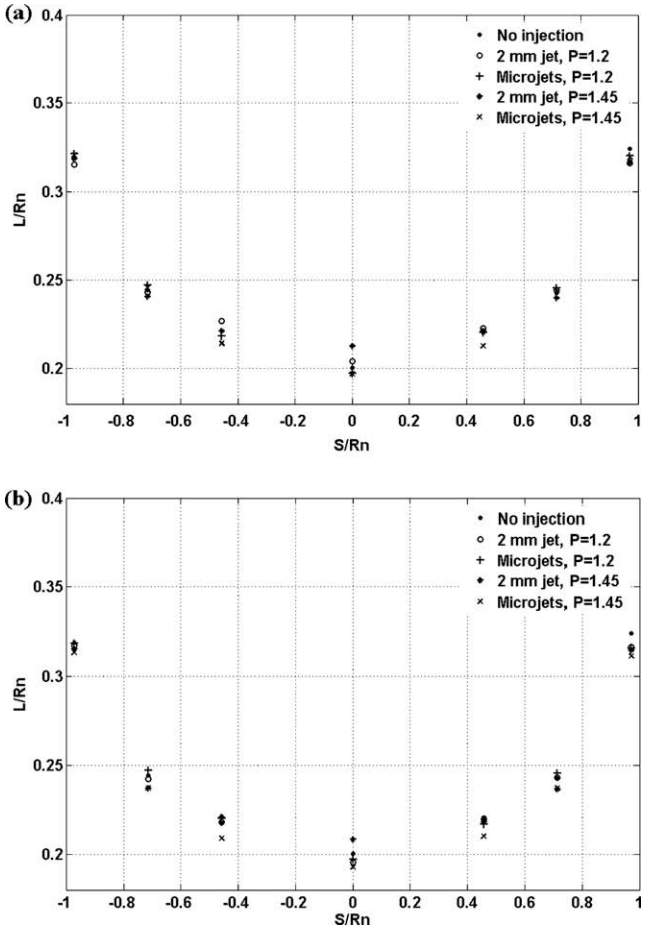

Fig. 11. Shock standoff distance normalized with *Rn* along the model surface in the nose region: (a) with and without nitrogen injection, (b) with and without helium injection.

the other array. When the jets are farther they almost behave as separate jets for a longer distance and thus do not lose their momentum. This has been confirmed from the visualizations also.

5.5. Qualitative inferences from visualization

The aerodynamic forces and moments on the blunt body are mainly due to the surface pressure distribution. The skin friction is negligible in comparison with pressure based forces. If the injection of the fluid could alter the pressure distribution, there will be a change in the overall aerodynamic characteristics. If the fluid is injected with very high momentum it can push the bow shock forward and reattach on the surface at a significant distance from the stagnation point so that there is a reasonable dead air region, where the pressure is very low. This leads to a reduction in drag, although the strong reattachment in such cases will be accompanied with a reattachment shock where the heat transfer and pressure is increased. But when the mass is injected with substantially low momentum there is no significant change in shock standoff distance. The dead air region is also very small and thus it can be expected that there is no significant change in the overall aerodynamic characteristics. Fig. 12 shows the time resolved schlieren images of the flow for the cases with 2 mm jet and corresponding micro jets, with and without nitrogen injection showing three frames (300 μs) during the steady time of the freestream. During the test time the external flow field appears steady with injection (external flow field looks very much the same for all the frames shown). It can be seen from the visualizations that the shock structure of the flow is not affected by the injection. This can be quantified by measuring the shock standoff distances from the model surface, from the schlieren images. Fig. 11 shows the shock standoff distance L (normalized with Rn) as a function of S/Rn for the different cases of with and without coolant injection (corresponding to 2 mm orifice).

It is seen that there is not much difference in the shock standoff distances between the different cases shown. There is a maximum percentage difference of around 5% at the stagnation point with the injection of a single jet with $P = 1.45$ with both helium and nitrogen. It can be seen from the schlieren images that for this case the jet just touches the bow shock and slightly disturbs the shock structure in the stagnation zone. With a single jet injection at $P = 1.2$ also the jet can be seen moving away from the orifice for a considerable distance, but has not considerably disturbed the bow shock. For the micro-jet injection it can be seen that the coolant mass is almost confined to the boundary layer. It almost spreads instantaneously over the surface from the point it is injected, leaving no significant region of dead air and reattachment, and thus not affecting the surface pressure distribution. This is a clear indication that with array of micro-jets there is no significant change in any aerodynamic force. Because the main flow is steady as seen from the visualization, the unsteadiness observed in heat transfer rates due to injection must be due to the unsteadiness in the boundary layer flow, where the coolant spreads. Although this is not clearly seen in the visualizations with the injection of single

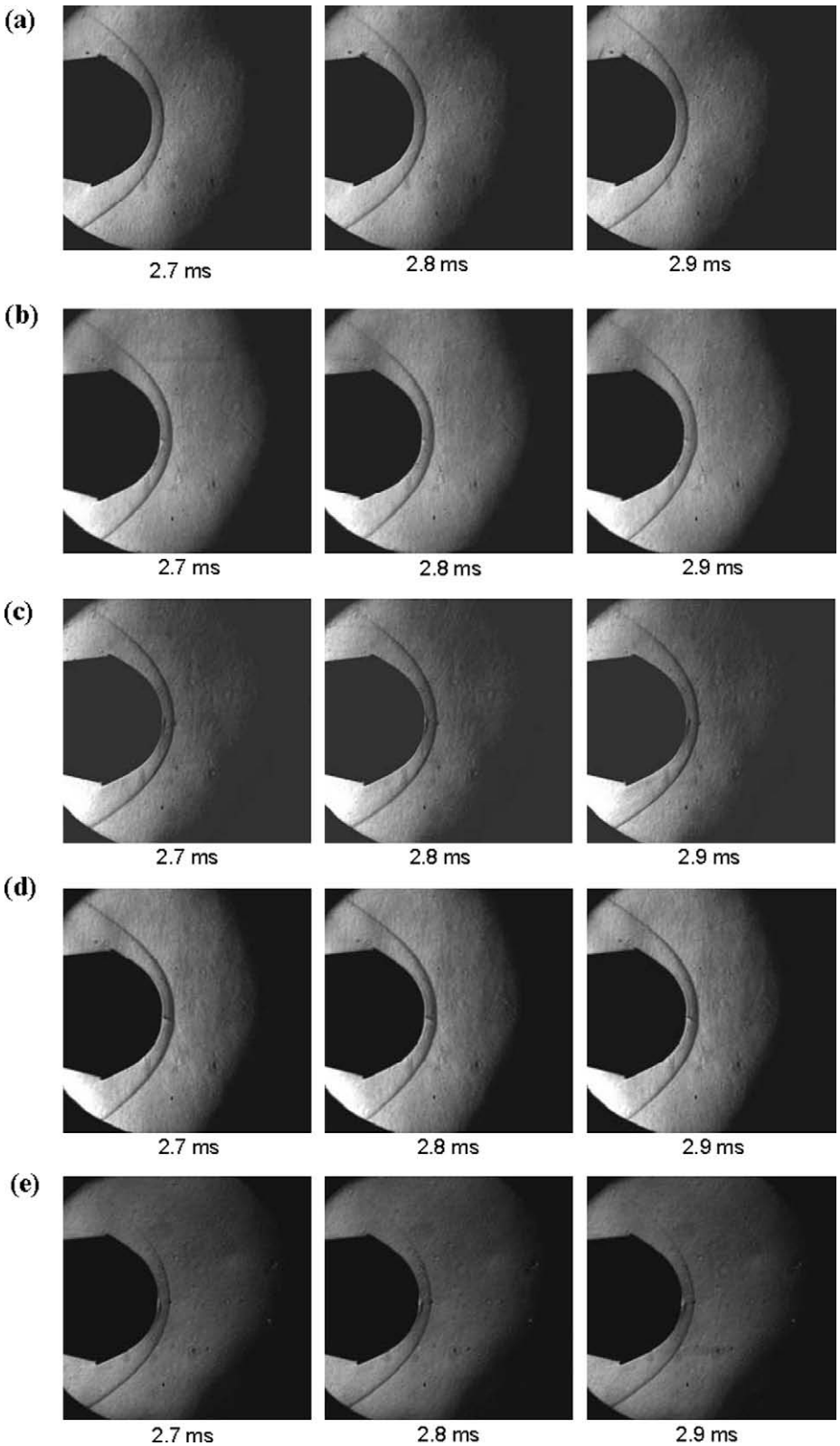

Fig. 12. Schlieren images of the flow field during steady time with and without nitrogen injection: (a) without injection, (b) 2 mm jet, $P = 1.2$, (c) micro jets $P = 1.2$, (d) 2 mm jet, $P = 1.45$, (e) micro jets $P = 1.45$.

jet, with micro-jets the unsteadiness can be seen at the injection zone, where the coolant flow shows differences during the different time frames shown. Fig. 13 shows the schlieren images at 2.8 ms for the cases with 0.9 mm jet and corresponding arrays, with nitrogen injected with $P = 1.45$. With the array from $5 \times 5\ mm^2$ the individual jets can be clearly seen coming out of the orifice. With closely spaced jet array the jets can be seen not carrying much forward and appear to merge shortly after coming out of orifice, although the image is not very clear. But with those for 46 micro jets corresponding to 2 mm area, it is clear from the

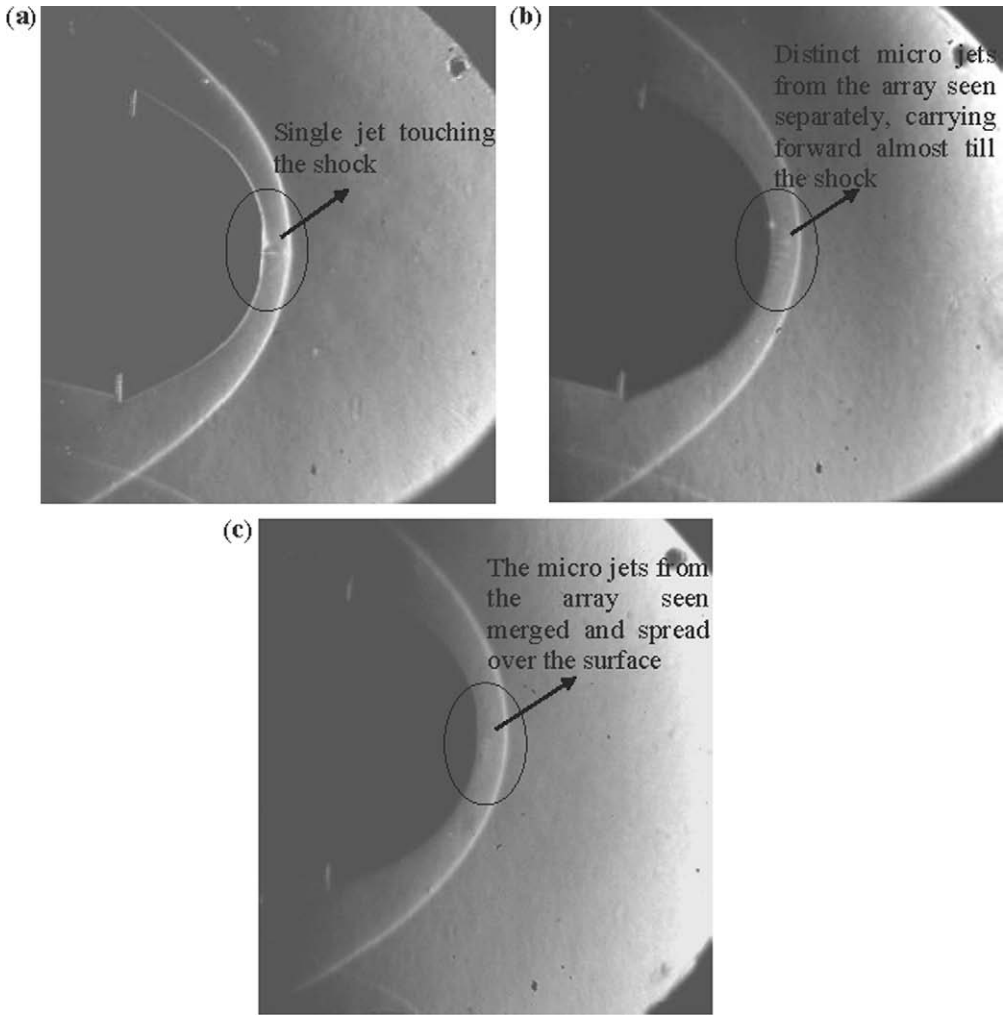

Fig. 13. Schlieren images of the flow field during steady time (2.8 ms frame) with nitrogen injection at $P = 1.45$, for (a) 0.9 mm jet, (b) equivalent array of micro jets from 5×5 mm^2, (c) equivalent array of micro jets from 3×3 mm^2.

visualizations that the jets merge as soon as they come out of the orifice, thus losing the momentum.

6. Conclusion

The film cooling effectiveness by the injection of coolant mass as a single jet and as an array of micro-jets of same effective area, from the stagnation zone of a hypersonic blunt body has been investigated experimentally in IISc hypersonic shock tunnel and a comparison has been made between their percentage reductions in heat transfer rates. Nitrogen and helium are the coolant gases injected and the mass flow rate of each of the coolant is varied by varying the injection pressure ratio and the injection area. Essentially the effect of momentum flux of the jet (varying jet diameter d_j and by splitting the single jet into micro jets whose spacing is varied), mass flux of the jet (varying P/varying injection area) and the molecular weight of the coolant on film cooling performance is investigated. The following conclusions are made from the experiments.

1. It is observed that the cooling performance of the array of closely spaced micro-jets is much better than the corresponding single jet almost over the entire surface.
2. The cooling effectiveness of the array of micro-jets in comparison with the corresponding single jet can be clearly seen in the vicinity of the stagnation zone. In the region close to stagnation point (where the first sensor is placed) the reduction in Stanton number with micro jets is up to 40% with nitrogen as coolant, and 30% with helium as coolant, as compared to the case without any injection. For the corresponding single jet case, in the same location, either there is no significant heat transfer reduction, or up to 10% increase in Stanton number is observed (compared with the case without any injection).
3. As the distance from the stagnation zone increases the differences in percentage reduction in Stanton number between the cases of single jet and micro jets becomes lesser. This shows that for the same mass flow rate, if the momentum flux of the coolant is reduced, the film cooling performance gets better.
4. The heavier gas nitrogen is found to have a better cooling performance in the vicinity of stagnation zone than helium. The cooling performance of helium gets better far away from stagnation zone, but over all the heavier gas is found effective in cooling.
5. The increase in pressure ratio, which essentially increases the mass flow rate, generally leads to better cooling performance, although with a single jet injection or for array of micro jets spaced far away, the trend is reversed at the jet reattachment zone.

6. From the visualizations it is seen that there is not much alteration in the external flow structure, but the injection of the coolant essentially alters the boundary layer characteristics. The aerodynamic forces certainly cannot change significantly by injecting the coolant as an array of micro-jets with such low momentum fluxes.
7. The unsteadiness in the heat transfer value with coolant injection is mainly due to the unsteadiness in the boundary layer filled with coolant mass, as the external flow is steady as seen from the visualizations.
8. The effect of momentum reduction is not mainly by the increased viscous activity in the orifice wall boundary layer by reducing the orifice diameter, but dominantly due to viscous interaction between individual jets of the array. This is verified by comparing the cooling performance of two different arrays. The array with jets separated apart almost shows the same reduction in heat transfer as that of a single jet, whereas that with closely spaced jets leads to a better cooling.

Acknowledgements

The support rendered by Dr. K. Satheesh, Mr. D. Mahapatra, Mr. Srisha Rao, and Mr. Jeevan during the course of this work is sincerely acknowledged.

References

[1] F.I. Peter, B.K. Donn, High-speed aerodynamics of several blunt cone configurations, J. Spacecraft Rockets 24 (1987) 127–132.
[2] P.J. Finley, The flow of a jet from a body opposing a supersonic freestream, J. Fluid Mech. 26 (1966) 337–368.
[3] Balla Venukumar, G. Jagadeesh, K.P.J. Reddy, Counterflow drag reduction by a supersonic jet for a blunt body in hypersonic flow, Phys. Fluids 18 (2006) 118104.
[4] J.S. Shang, J. Hayes, K. Wurtzlet, W. Strang, Jet-spike bifurcation in high-speed flows, AIAA J. 39 (2001) 1159–1165.
[5] C.H.E. Warren, An experimental investigation of the effect of ejecting a coolant gas at the nose of a bluff body, J. Fluid Mech. 8 (1960) 400–417.
[6] Sahoo Niranjan, Vinayak Kulkarni, S. Saravanan, G. Jagadeesh, K.P.J. Reddy, Film cooling effectiveness on a large angle blunt cone flying at hypersonic Mach number, Phys. Fluids 17 (2005) 036102.
[7] J.A. Fay, F.R. Riddell, Theory of stagnation point heat transfer in dissociated air, J. Aeronaut. Sci. 25 (1958) 73–85.
[8] L. Lee, Laminar heat transfer rate over blunt nosed body at hypersonic speeds, Jet Propulsion 26 (1956) 259–269.
[9] D.L. Schultz, T.V. Jones, Heat transfer measurements in short-duration hypersonic facilities, AGARDograph-AG-165, 1973.
[10] G. Jagadeesh, N.M. Reddy, K. Nagashetty, K.P.J. Reddy, Fore body convective hypersonic heat transfer measurements over large angle blunt cones, J. Spacecraft Rockets 37 (1) (2000) 137–139.
[11] R.J. Moffat, Describing the uncertainties in experimental results, Exp. Therm. Fluid Sci. 1 (1988) 3–17.
[12] K. Satheesh, G. Jagadeesh, K.P.J. Reddy, High-speed schlieren facility for visualization of flow fields in hypersonic shock tunnels, Curr. Sci. 92 (2007) 56–60.